Bit Error Probability Analysis of UWB Communications with a Relay Node

Zolfa Zeinalpour-Yazdi, *Student Member, IEEE*, Masoumeh Nasiri-Kenari, *Member, IEEE*, and Behnaam Aazhang, *Fellow, IEEE*

***Abstract*—In this paper, the extension of cooperative communication to the context of TH-UWB is investigated. In particular, the average bit error probability (BEP) is provided for cooperative TH-UWB systems with decode-and-forward relaying protocol. In the considered relay network, UWB links among the nodes are modeled according to IEEE 802.15.4a standards. Our methodology is based on computing the Characteristic Function (CF) of the decision variable at the destination terminal. We use Gaussian quadrature numerical method to approximate the CF of interference component appeared in decision variable term. This technique permits to predict the system performance in different IEEE 802.15.4a defined channels with high accuracy and reasonable complexity. Numerical results show that significant improvement in the BEP of impulse radio UWB system is obtained by adding a relay node. The analytical expressions are also validated by computer simulations which confirm the accuracy of the approximations used in obtaining the BEP.**

***Index Terms*—Relay channel, ultra-wideband (UWB), IEEE 802.15.4a, Gaussian quadrature rule, error analysis.**

I. Introduction

ULTRA-WIDEBAND (UWB) has been widely envisioned as an excellent candidate for high-speed, low cost indoor wireless communications [1]. According to the Federal Communications Commission (FCC) rule, UWB should operate at a transmit power of at most $-41.3\mathrm{dBm/MHz}$ to avoid the interference with existing narrow-band communication systems. Due to this limitation, UWB system faces major design challenges in achieving wide coverage while assuring an adequate system performance [2]. Therefore, it is greatly necessary to find some kinds of efficient ways to enhance the system performance. Recently, cooperative diversity has emerged as an effective scheme to overcome multipath fading and thus to improve the quality of service in wireless networks [3]. The fundamental idea of the cooperative strategy is to transport data through multiple nodes such that these nodes work cooperatively to improve the overall network performance [4].

The simplest example of a cooperative network is a relay network, which was first introduced by Van der Meulen [5]. The effectiveness of the user relaying on network performance improvement from different aspects such as error probability [6], [7], achievable rate region [8], [9], and outage behavior [10], [11] has been demonstrated. Most of these results have been derived for transmission in a narrow-band flat fading channel while the UWB channel model does not follow flat fading statistics. The IEEE 802.15.3a and 4a task groups have proposed channel models for UWB systems [12] based on the Saleh-Valenzuela model where multipath components arrive in the random number of clusters and rays in each cluster. UWB has been a subject of extensive study in the literature [13], [14] (and references therein), where some of them analyze the performance of the system under the above realistic multipath channel models. However, most of the above contributions rely on either numerical approximations to perform the analysis or on simplifications for modeling the wireless channel; there are few works that provide analytical formulation for the BEP of UWB without significantly simplifying the channel model. In [15], an exact and more realistic method to model the statistics of multiple access interference (MAI) for TH-PPM, TH-PAM and DS-PAM schemes in AWGN channel and also in multipath channel (using a simplified channel model) with a single correlator receiver has been presented. The BEP of DS-PPM system for the tapped delay line channel model with lognormal fading gains and a single correlator receiver has been derived in [16]. The results in [16] show that the Gaussian approximation method underestimates the BEP value in high SNR range. In [17], an analytical framework for deriving BEP formula was developed for a simple correlator receiver, by treating an IEEE 802.15.3a channel as a two-dimensional augmented cluster process while the effect of the pulse function is simplified as a rectangular window and neither ISI nor MAI is considered. Although the viewpoint in [17] is general, the analysis for channel related statistical quantities, which relies on calculating the expectation of shot-noise random variables, is still based on the assumption of a Poisson cluster arrival process. Moreover, the inherent assumption of a Poisson cluster arrival process inevitably limits the application to extended UWB channel models. The path arrival statistics in an IEEE 802.15.4a channel is generalized from that of an IEEE 802.15.3a channel by setting a random cluster number and employing a mixture of two exponential distributions for the ray inter-arrival times. It is evident that previous works assuming Poisson arrival processes will fail to be applicable. Although the above work was extended in [18] for IEEE 802.15.4a channel models, the obtained

Manuscript received March 16, 2009; revised July 24, 2009, September 16, 2009, and September 27, 2009; accepted September 30, 2009. The associate editor coordinating the review of this paper and approving it for publication was D. I. Kim.

Z. Zeinalpour-Yazdi and M. Nasiri-Kenari are with the Department of Electrical Engineering, Sharif University of Technology, Tehran, Iran (e-mail: zeinalpour@ee.sharif.edu).

B. Aazhang is with the Department of Electrical and Computer Engineering, Rice University , Houston, TX 77251 USA and Center for Wireless Communication at University of Oulu, Finland.

Digital Object Identifier 10.1109/TWC.2010.02.090383

analytical results are not adequate for channel higher-order cross moments of interests. A semi-analytical expressions have been also obtained to approximate the error rate of the coded IR-UWB transmission for both coherent and noncoherent reception according to the IEEE 802.15.4a standard in [19].

The utility of cooperative diversity with UWB systems was outlined in a few contributions [20], [21], [2]. Abou-Rjeily *et al.* has extended the decode-and-forward (DF) and amplify-and-forward (AF) cooperative diversity schemes to the context of impulse radio UWB in [20] and [21], respectively. Specifically, they have presented the construction of a family of space-time codes which are suitable for TH-UWB with AF and DF protocols. In [2], symbol-error-rate (SER) performance analysis and optimum power allocation of MB-OFDM-UWB systems with DF cooperative protocol have been derived, and the upper bound on the capacity of this protocol has been addressed in [22]. Altogether, research for cooperative networks with UWB transmission is still largely unexplored, especially for the multipath fading propagation. The objective of this paper is to evaluate the BEP performance of the classical TH-PPM-UWB system in a relay networks with realistic UWB links specified by the IEEE 802.15.4a standard. We apply the characteristic function (CF) method to calculate the exact BEP. In computing the CF of interference, we face with a complicated integral, where we use a powerful analytical tool, namely the Gaussian quadrature rules (GQRs), for its numerical evaluation. Particularly, we find a suitable Gaussian quadrature method for each different environmental scenario defined in IEEE 802.15.4a model. While this approach shows a good agreement with simulated curves, it requires a limited computational complexity and provides a saving in computation time.

The rest of this paper is organized as follows: Section II describes the UWB channel model and the relaying protocol considered in our analysis. The exact expression for the average probability of bit error and its approximation are then derived in Section III. Finally, we evaluate and discuss the results in Section IV and conclude the paper in Section V.

II. System Description

We consider a wireless network composed of source-destination (link 1), source-relay (link 2), and relay-destination (link 3) links. Data is transmitted from the source terminal S to the destination terminal D with the assistance of the relay terminal R. The relay node assists the source-destination communication by decoding the source transmission and forwarding the message in order to increase the reliability of decoding at the destination terminal. The cooperation strategy consists of two time slots with equal time intervals, in which the source broadcasts its signal to destination and relay nodes during the first time slot, and in the second time slot, the source is silent and only the relay node communicates with the destination. The channel between the nodes are assumed mutually independent and identically distributed based on the Saleh-Valenzuela (S-V) model [23] with slight modifications, as described in the following part. In the following, we will describe this UWB channel model and the signal model for our scenario.

A. Channel Model

We adopt the multipath channel model specified by the IEEE 802.15.4a group for the performance evaluation of the physical layer of UWB [12]. The impulse response of this model can be expressed mathematically by [12]

$$h(t) = \widetilde{\beta} \sum_{\ell=0}^{L-1} \sum_{m=0}^{M-1} a_{m,\ell} e^{j\phi_{m,\ell}} \delta(t - T_\ell - \tau_{m,\ell}), \qquad (1)$$

where $a_{m,\ell}$ is the gain of the mth path in the ℓth cluster. T_ℓ and $\tau_{m,\ell}$ represents the cluster and ray arrival times, respectively. The factor $\widetilde{\beta}$ jointly models the pathloss and shadowing (the effects of the transmit and the receive antennas are ignored in our model). The number of clusters L is assumed to be Poisson-distributed. M is the number of paths in each cluster. The actual value of M depends on the required dynamic range of the model. The paths considered can be the ones with a power within x dB of the peak power or the paths which arrive within the specified time. The cluster arrival times are given by a Poisson processes

$$p(T_l|T_{l-1}) = \Lambda \exp\left[-\Lambda\left(T_l - T_{l-1}\right)\right], \quad l > 0, \qquad (2)$$

where Λ is the cluster arrival rate. To have a best fitting for most of the environment ray arrival times are modeled with mixtures of two Poisson processes as follows

$$\begin{aligned} p(\tau_{k,\ell}|\tau_{k-1,\ell}) \;=\; & \beta\lambda_1 \exp\left[-\lambda_1\left(\tau_{k,\ell} - \tau_{k-1,\ell}\right)\right] \\ & +(1-\beta)\lambda_2 \exp\left[-\lambda_2(\tau_{k,\ell} - \tau_{k-1,\ell})\right],\ k>0 \end{aligned} \qquad (3)$$

where β is the mixing factor, while λ_1 and λ_2 are the ray arrival rates. By definition $\tau_{0,\ell} = 0$.

The distribution of the small-scale fading, *i.e.*, $a_{m,\ell}$ in (1), is Nakagami with parameter $m_{m,\ell}$, which is modeled as a lognormally distributed random variable and finally the phase $\phi_{m,\ell}$ is considered as a uniformly distributed random variable from the range $[0, 2\pi]$. The detail of joint probabilistic model of these parameters is tabularized in [12].

B. Signal Model

Throughout this paper, we focus on the TH-PPM system. The signaling interval T_s is composed of N_f frames of duration T_f. During the transmission of each information symbol, a UWB pulse $p(t)$ which has ultra-short duration T_p and conveys information is repeated over these adjacent frames. This N_f-fold pulse repetition increases the energy per symbol or, for a given symbol energy, it reduces the energy of the individual pulses. Each frame contains N_h subinterval of T_c seconds. So by using a TH sequence each pulse position can be time-shifted at multiples of the chip duration (T_c), which allows multiple access without catastrophic collisions. Note that as we stated previously, in the considered cooperation Protocol during time slot I, S transmits while R and D listen and during time slot II, S is silent, while R decodes and forwards its received signal to D. A typical TH-PPM UWB signal transmitted from the source (in the first time slot) and relay node (in the second time slot) can be expressed mathematically as

$$s_i(t) = \sum_{j=-\infty}^{+\infty} \sum_{n=0}^{N_f-1} \sqrt{E_i}\, p(t - jT_s - nT_f - c_{j,n}^i T_c - \delta d_j^i) \qquad (4)$$

Here, the index $i \in \{s, r\}$ determines the transmitted signals from the source and the relay nodes, respectively. E_i is the energy of the transmitted pulse which is related to the bit energy E_{b_i} with $E_i = E_{b_i}/N_f$. $c^i_{j,n}$ is the pseudorandom sequence which provides additional time shift of $c^i_{j,n}T_c$ second to each transmitted pulse. The elements of this sequence are i.i.d random variables which uniformly take on integer values in the interval $[0, N_h-1]$. $d^i_j \in \{0, 1\}$ represents the jth binary data bit of transmitter i. In PPM modulation considered, no additional time shift modulates the pulse $p(t)$ when the data bit is 0, and a time shift δ is added to $p(t)$ when the data bit is 1. We also assume that $T_c = T_p + \delta$. Now using (1) and (4), the received signals at the relay node ($r_{sr}(t)$) and destination (in the first and second time slots ($r_{sd}(t)$ and $r_{rd}(t)$) can be written as (5)–(7), shown at the bottom of the page. In these equations, for notational simplicity, we have inserted the parameter $\alpha^{(i)}_{k,\ell}$ instead of $\widetilde{\beta}^{(i)}a^{(i)}_{k,\ell}e^{j\phi^{(i)}_{k,\ell}}$. $n_r(t)$, $n_{d_I}(t)$ and $n_{d_{II}}(t)$ are the complex additive white Gaussian noise components with zero mean and variance N_0 at the relay node and destination terminal in time slot I and II, respectively. The other parameters have been defined in (1) and (4). Note that in this protocol in both time slots we deal with a single user channel. Therefore we can assume $c^k_{j,n} = 0$. However, TH sequence might be still employed to help smoothening the power spectral density of the transmitted signals [24].

Our aim is the detection of the information bit d^s_j based on the observation of the signal received in the interval $[jT_s, (j+1)T_s)]$. Without loss of generality, we concentrate on the detection of d^s_0 and drop the symbol index 0. Also the frame length is chosen to be sufficiently large ($T_f > (N_h - 1)T_c + Tp + T_m + \delta$) to preclude intersymbol and intrasymbol interferences [14], [25], where $T_m = \max(T_{m_1}, T_{m_2}, T_{m_3})$ in which T_{m_i} is the maximum excess delay spread of link i.

Because UWB signals occupy large bandwidth and the channel is extremely frequency-selective, the received signals contain a significant number of resolvable multipath components. To exploit the multipath diversity, a rake receiver is considered. Because of complexity constraints, however, the rake receiver processes only a subset of the total number of received multipath components [14]. It is assumed that an K'-finger rake receiver at the destination will capture K' rays from the first clusters of $S-D$ UWB links during the first transmission time slot and during the second time slot they are coincident to the $R-D$ UWB link [26]. The template waveforms used in the correlators of the destination in time slots I and II are given respectively as

$$v_{sd,k} = \alpha^{(1)*}_{k,0}\sum_{n=0}^{N_f-1} q(t - nT_f - c^s_n T_c - T^{(1)}_0 - \tau^{(1)}_{k,0})$$
$$v_{rd,k} = \alpha^{(3)*}_{k,0}\sum_{n=0}^{N_f-1} q(t - nT_f - c^r_n T_c - T^{(3)}_0 - \tau^{(3)}_{k,0}) \quad 0 \le k \le K'-1 \tag{8}$$

For the relay node, the template waveforms used are

$$v_{sr,k} = \alpha^{(2)*}_{k,0}\sum_{n=0}^{N_f-1} q(t - nT_f - c^s_n T_c - T^{(2)}_0 - \tau^{(2)}_{k,0}) \quad 0 \le k \le K'-1 \tag{9}$$

where $q(t) = p(t) - p(t-\delta)$. Notice that we assume that the channel fading coefficients are quasi static during at least one symbol duration. This assumption is reasonable as the UWB channel is slow time varying in most PAN applications [16].

III. Performance Analysis of PPM-TH UWB Communication with a Relay Node

In this section we investigate the bit error probability performance of the system in a semi-analytical way by evaluating the desired signal as well as the interference and noise terms one by one. The key idea is to compute the characteristic functions of the noise and interference terms (Section III-B) which are then used in deriving the BEP of the considered network in Section III-C. Finally in Section III-D we establish an approximation approach, which allows us to obtain a simpler performance formulation of the system.

We now proceed to form the decision variable. At destination, the receiver combines the data transmitted via two time slots to increase system performance. The output decision variables of the destination rake receiver in time slots I and II, $\hat{Z}_{sd}$ and $\hat{Z}_{rd}$, are given by

$$\hat{Z}_{sd} = \sum_{k=0}^{K'-1}\int_0^{T_s} r_{sd}(t)v_{sd,k}(t)dt = \int_0^{T_s} r_{sd}(t)\sum_{k=0}^{K'-1}\sum_{n=0}^{N_f-1}\alpha^{(1)}_{k,0}q(t - nT_f - T^{(1)}_0 - \tau^{(1)}_{k,0}) \tag{10}$$

$$\hat{Z}_{rd} = \sum_{k=0}^{K'-1}\int_0^{T_s} r_{rd}(t)v_{rd,k}(t)dt = \int_0^{T_s} r_{rd}(t)\sum_{k=0}^{K'-1}\sum_{n=0}^{N_f-1}\alpha^{(3)}_{k,0}q(t - nT_f - T^{(3)}_0 - \tau^{(3)}_{k,0}) \tag{11}$$

$$r_{sr}(t) = \sum_{\ell=0}^{L_2-1}\sum_{k=0}^{K_2-1}\sum_{j=-\infty}^{+\infty}\sum_{n=0}^{N_f-1}\alpha^{(2)}_{k,\ell}\sqrt{E_s}p(t - jT_s - nT_f - \delta d^s_j - c^s_{j,n}T_c - T^{(2)}_\ell - \tau^{(2)}_{k,\ell}) + n_r(t) \tag{5}$$

$$r_{sd}(t) = \sum_{\ell=0}^{L_1-1}\sum_{k=0}^{K_1-1}\sum_{j=-\infty}^{+\infty}\sum_{n=0}^{N_f-1}\alpha^{(1)}_{k,\ell}\sqrt{E_s}p(t - jT_s - nT_f - \delta d^s_j - c^s_{j,n}T_c - T^{(1)}_\ell - \tau^{(1)}_{k,\ell}) + n_{d_I}(t) \tag{6}$$

$$r_{rd}(t) = \sum_{\ell=0}^{L_3-1}\sum_{k=0}^{K_3-1}\sum_{j=-\infty}^{+\infty}\sum_{n=0}^{N_f-1}\alpha^{(3)}_{k,\ell}\sqrt{E_r}p(t - jT_s - nT_f - \delta d^r_j - c^r_{j,n}T_c - T^{(3)}_\ell - \tau^{(3)}_{k,\ell}) + n_{d_{II}}(t) \tag{7}$$

The receiver finally combines these two variables with a factor λ which can control the near-far effect (consists of pathloss) and makes the final decision variable $\hat{Z}$ as

$$\hat{Z} = \hat{Z}_{sd} + \lambda \hat{Z}_{rd}. \tag{12}$$

Sendonaris *et al.* have refereed to this detector as the λ-MRC detector [27]. The receiver makes a decision on 0 if $Z \triangleq \Re\{\hat{Z}\} > 0$, and 1 if $Z < 0$. Note that our receiver is not optimum (because of the self interference arising from UWB multipath channel) and it extracts the energy from the first K' paths, which are the strongest paths of the channel especially in a LOS environment. In the following we derive the statics and characteristic function of $Z_{sd} \triangleq \Re\{\hat{Z}_{sd}\}$. The characteristic function of $Z_{rd} \triangleq \Re\{\hat{Z}_{rd}\}$ can be computed, similarly. Then, using these results the bit error probability of the relay network with UWB links will be carried out.

A. Z_{sd} Statics

Substituting (6) in (10), gives the output decision variables of the destination receiver in time slots I shown at the bottom of the page. As seen, $\hat{Z}_{sd}$ can be decomposed into three terms, i.e., desired signal , self multipath interference, and noise. For notational simplicity, in the following subsections we drop the superscript (sd).

1) Desired Signal: With the definition

$$R(x) \triangleq \int_{-\infty}^{+\infty} p(t-x)q(t)dt, \tag{14}$$

the useful signal component can be written as

$$D = N_f\sqrt{E_s}\sum_{k=0}^{K'-1}\left|\alpha_{k,0}^{(1)}\right|^2 \cdot R(\delta d^s) \tag{15}$$

2) Self Multipath Interference: In a rake receiver, each finger is to capture one resolvable path. So the self interference (SI) in each finger comes from the other paths. More specifically the correlation between the correspondent template waveform at each finger of the rake receiver with all the received multipath components (all rays in the 0^{th} to $L_1 - 1^{th}$ clusters) are examined. One term is desired signal and the sum of the rest terms are treated as the SI of that finger. Then, the total self interference ($\hat{I}_s$) is the sum of the SI of all fingers. Note that the frame length T_f ensures that SI does not contain the symbols transmitted in the other frames and from (13) it is equal to

$$\hat{I}_s = N_f\sqrt{E_s}\sum_{k=0}^{K'-1}\sum_{k_1=0,k_1\neq k}^{K_1-1}\alpha_{k_1,0}^{(1)}\alpha_{k,0}^{(1)^*}R(\tau_{k_1,0}^{(1)} - \tau_{k,0}^{(1)} + \delta d^s)$$
$$+N_f\sqrt{E_s}\sum_{k=0}^{K'-1}\sum_{\ell_1=1}^{L_1-1}\sum_{k_1=0}^{K_1-1}\alpha_{k_1,\ell_1}^{(1)}\alpha_{k,0}^{(1)^*}R(T_\ell^{(1)}+\tau_{k,\ell}^{(1)}+\delta d^s-T_0^{(1)}-\tau_{k,0}^{(1)}) \tag{16}$$

The first term in the right hand of (16) corresponds to the interference of the 0^{th} cluster and the second term is related to the other clusters. Based on the parametrization for different environmental scenarios defined in IEEE 802.15.4a model in [12], the arrival time between the rays in different clusters is typically more than the pulse duration T_p, which is less than a nanosecond. Since $R(x)$ is zero out of $[-T_p, T_p + \delta]$, with a good approximation we can assume that the second term of the above equation is zero. With the same reasoning, we can conclude that $R(\tau_{k_1,0}^{(1)} - \tau_{k,0}^{(1)} + \delta d^s) = 0$ for $|k_1 - k| \neq 1$, which means that the rays (in the same clusters) that are not adjacent come in the intervals which are larger than the pulse duration. So the real part of (16) is simplified as

$$I_s \triangleq \Re\{\hat{I}_s\} = \sum_{k=0}^{K'-1} I_{s_k} \tag{17}$$

where

$$I_{s_k} = N_f\sqrt{E_s}\Big(\Re\{\alpha_{k+1,0}^{(1)}\alpha_{k,0}^{(1)^*}\}R(\nu_{k+1,0}^{(1)}+\delta d^s) + \Re\{\alpha_{k,0}^{(1)}\alpha_{k+1,0}^{(1)^*}\}R(-\nu_{k+1,0}^{(1)}+\delta d^s)\Big) \quad 0 \le k < K'-2$$
$$I_{s_{K'-1}} = N_f\sqrt{E_s}\left(\Re\{\alpha_{K',0}^{(1)}\alpha_{K'-1,0}^{(1)*}\}R(\nu_{K',0}^{(1)}+\delta d^s)\right) \tag{18}$$

To derive this equation, we have replaced the arrival time of the mth ray in the ℓth cluster $\tau_{m,\ell}^{(1)}$ with $\sum_{j=1}^{m}\nu_{j,\ell}^{(1)}$, where $\nu_{j,\ell}^{(1)}$ is the interarrival time between rays j and $j-1$ in the ℓth cluster [28]. It can be easily observed that $\nu_{j,\ell}^{(1)}$s are i.i.d random variables with the distribution defined in (3).

3) AWGN: The noise component $\hat{\eta}$ in the output of the rake receiver is given by

$$\hat{\eta} = \int_0^{T_s} n_{d_I}(t)\sum_{k=0}^{K'-1}\alpha_{k,0}^{(1)^*}\sum_{n=0}^{N_f-1}q(t-nT_f-T_0^{(1)}-\tau_{k,0}^{(1)})dt \tag{19}$$

we readily obtain $\mathbb{E}\{\hat{\eta}\} = 0$ and $\sigma_{\hat{\eta}}^2 = 2N_fR(0)N_0\sum_{k=0}^{K'-1}\left|\alpha_{k,0}^{(1)}\right|^2$. If we define η as the real part of $\hat{\eta}$, then η will be also Gaussian variable with zero mean and variance of

$$\sigma_\eta^2 = \frac{1}{2}\sigma_{\hat{\eta}}^2 = N_fR(0)N_0\sum_{k=0}^{K'-1}\left|\alpha_{k,0}^{(1)}\right|^2 \tag{20}$$

$$\begin{aligned}\hat{Z}_{sd} &= \int_0^{T_s}\sum_{\ell_1=0}^{L_1-1}\sum_{k_1=0}^{K_1-1}\sum_{n=0}^{N_f-1}\sum_{k=0}^{K'-1}\sqrt{E_s}\alpha_{k_1,\ell_1}^{(1)}\alpha_{k,0}^{(1)^*}p(t-nT_f-\delta d^s-T_\ell^{(1)}-\tau_{k,\ell}^{(1)})q(t-nT_f-T_0^{(1)}-\tau_{k,0}^{(1)})dt \\ &+ \int_0^{T_s} n_d(t)\sum_{k=0}^{K'-1}\alpha_{k,0}^{(1)^*}\sum_{n=0}^{N_f-1}q(t-nT_f-T_0^{(1)}-\tau_{k,0}^{(1)})dt \\ &= D^{(sd)} + \hat{I}_s^{(sd)} + \hat{\eta}^{(sd)}\end{aligned} \tag{13}$$

B. Characteristic Function Analysis

1) CF of Self Interference (I_s): The channel model in [12] was accepted by the standardization group, IEEE 802.15.4a, as the model for the evaluation of the proposals for UWB standardization activities, which well models a real UWB channel. As we stated previously, this model contains multiple clusters (of rays) with random cluster-starting times, hence the power decaying profile (PDP) is segmented. Furthermore, the channel gain is modeled as a Nakagami random variable multiplied by a lognormal variable to represent the shadowing effect. Therefore, it will be very complicated to compute the unconditional characteristic function of the self interference. In order to make the analysis theoretically tractable, we assume that the channel gains are independent from their arrival times and the corresponding PDP can be defined by the product of two decaying exponential functions independent of the cluster and ray arrival times. We compute the characteristic function of the self interference conditioned on the channel gains, and then the conditional BEP is obtained in the next section. Finally, to derive the unconditional bit error probability we take average from the conditional BEP using Monte Carlo method. For notational simplicity, we collectively denote the channel gains $\{\alpha_{k,0}^{(1)}\}_{k=0}^{K'}$ as $\underline{\boldsymbol{\alpha}}^{(1)}$ in this section. By conditioning upon $\underline{\boldsymbol{\alpha}}^{(1)}$ and d_s, the interference term $I_{s_k}(k=0,...,K'-1)$ is a function of only $\nu_{k+1,0}^{(1)}$. As $\{\nu_{k,0}^{(1)}\}_{k=0}^{K'}$ are independent random variables, so $\{I_{s_k}\}_{k=0}^{K'-1}$ are independent and we have

$$\Phi_{I_s|\underline{\boldsymbol{\alpha}}^{(1)},d_s}(w)=\mathbb{E}\Big\{e^{jwI_s}|\underline{\boldsymbol{\alpha}}^{(1)},d_s\Big\}=\prod_{k=0}^{K'-1}\mathbb{E}\Big\{e^{jwI_{s_k}}|\underline{\boldsymbol{\alpha}}^{(1)},d_s\Big\}$$
$$=\prod_{k=0}^{K'-1}\Phi_{I_{s_k}|\underline{\boldsymbol{\alpha}}^{(1)},d_s}(w) \tag{21}$$

where $\Phi_{I_{s_k}|\underline{\boldsymbol{\alpha}}^{(1)},d_s}$ for $0\le k<K'-2$ and $k=K'-1$ are given in (22) and (23), respectively. In these equations, from (3), $f_\nu(\nu)$ is equal to

$$f_\nu(\nu)=\beta\lambda_1 e^{-\lambda_1\nu}+(1-\beta)\lambda_2 e^{-\lambda_2\nu}. \tag{24}$$

Note that as $\{\nu_{k,0}^{(1)}\}_{k=0}^{K'}$ have identical probability distributions we have dropped their subscripts in the above equations. By defining

$$\tilde{U}(a_1,a_2,c_1,c_2)\triangleq\int_0^\infty e^{jw(a_1R(\nu+c_1)+a_2R(-\nu+c_2))}f_\nu(\nu)d\nu \tag{25}$$

we have

$$\Phi_{I_s|\underline{\boldsymbol{\alpha}}^{(1)},d_s}(w)=\tilde{U}\left(N_f\sqrt{E_s}\Re\{\alpha_{K',0}^{(1)}\alpha_{K'-1,0}^{(1)\,*}\},0,\delta d_s,0\right)$$
$$\cdot\prod_{k=0}^{K'-2}\tilde{U}\Big(N_f\sqrt{E_s}\Re\{\alpha_{k+10}^{(1)}\alpha_{k,0}^{(1)*}\},N_f\sqrt{E_s}\Re\{\alpha_{k,0}^{(1)}\alpha_{k+1,0}^{(1)\,*}\},\delta d_s,\delta d_s\Big) \tag{26}$$

It is obvious from (22) and (23) that a simple closed form solution for the CF of the self interference can not be obtained. Therefore the CF must be estimated by suitable numerical methods. Gaussian Quadrature Rules (GQR) are preferable as the integral can be approximated in the form of a finite series. This technique has been used in [15] to estimate the CF of a log normal variable with parameters μ and σ over a large range of these parameters. Our numerical evaluations have indicated that a single Gaussian quadrature method is not proper for all different environmental scenarios defined in IEEE 802.15.4a model, and in some cases the estimation errors are very high. That is for some environments such as office and outdoors (for both LOS and NLOS), $f_\nu(\nu)$ has significant value up to $\nu_{max}=5$ nsec; while for the residential environments (for both LOS and NLOS) it goes to zero at nearly $\nu_{max}=40$ nsec. So a special quadrature method, which approximates the CF of first case well, may not necessarily work quite well for the second group of the environments. In order to alleviate this problem, we have to find a suitable Gaussian quadrature method for each group.

By examining different Gaussian quadrature rules [29], we have found that Gauss-Legendre method can give good estimation for the first group (office and outdoor with LOS and NLOS scenarios), which yields to the term given in (27) at the bottom of the page.

To derive (27) we have truncated the integral to the interval $[a,b]=[0,\nu_{max}]$ (as $f_\nu(\nu)$ is nearly zero out of the interval $[0,\nu_{max}]$) and we have used the extension of the Gaussian

$$\Phi_{I_{s_k}|\underline{\boldsymbol{\alpha}}^{(1)},d_s}(w)=\int_0^\infty e^{jwN_f\sqrt{E_s}\left(\Re\{\alpha_{k+1,0}^{(1)}\alpha_{k,0}^{(1)\,*}\}R(\nu+\delta d^s)+\Re\{\alpha_{k,0}^{(1)}\alpha_{k+1,0}^{(1)}{}^{*}\}R(-\nu+\delta d^s)\right)}f_\nu(\nu)d\nu\quad 0\le k<K'-2 \tag{22}$$

$$\Phi_{I_{s_{K'-1}}|\underline{\boldsymbol{\alpha}}^{(1)},d_s}(w)=\int_0^\infty e^{jwN_f\sqrt{E_s}\Re\{\alpha_{K',0}^{(1)}\alpha_{K'-1,0}^{(1)\,*}\}R(\nu+\delta d^s)}f_\nu(\nu)d\nu, \tag{23}$$

$$\Phi_{I_{s_k}|\underline{\boldsymbol{\alpha}}^{(1)},d_s}(w)=\beta\lambda_1\sum_{i=1}^{N_p}w(y_i)\exp\left(jwN_f\sqrt{E_s}\Re\{\alpha_{k+1,0}^{(1)}\alpha_{k,0}^{(1)\,*}\}(R(y_i+\delta d^s)+R(-y_i+\delta d^s))-\lambda_1 y_i\right)$$
$$+(1-\beta)\lambda_2\sum_{i=1}^{N_p}w(y_i)\exp jwN_f\sqrt{E_s}\Re\{\alpha_{k+1,0}^{(1)}\alpha_{k,0}^{(1)\,*}\}\left(R(y_i+\delta d^s)+R(-y_i+\delta d^s)\right)-\lambda_2 y_i \tag{27}$$

quadrature rule to the arbitrary interval, namely

$$\int_a^b f(x)dx \approx \frac{b-a}{2}\sum_{i=1}^{N_p} w_i f\left(\frac{b-a}{2}x_i + \frac{b-a}{2}\right) \quad (28)$$

Therefore in (27),

$$y_i = \frac{b-a}{2}x_i + \frac{b-a}{2}, \quad (29)$$

where x_i is the ith zero of the Np order Legendre polynomial $P_{N_p}(x)$ (these roots occur symmetrically about 0) and the weight $w(y_i)$ in (27) is given by

$$w(y_i) = \frac{b-a}{2}w_i \quad (30)$$

here w_i is the corresponding weight of the abscissas x_i. For Legendre polynomials it equals

$$w_i = \frac{2(1-x_i^2)}{(N_p+1)^2 P_{N_p+1}^2(x_i)}. \quad (31)$$

The extension (28) becomes inaccurate (even for $N_p = 48$) when ν_{max} gets larger (for second group) and needs a very large value of N_p. To resolve this problem and find another suitable quadratic form for the second group we rewrite (22) as

$$\Phi_{I_{s_k}|\underline{\boldsymbol{\alpha}}^{(1)},d_s}(w) = \beta\int_0^\infty f_1(\nu)e^{-\nu}d\nu + (1-\beta)\int_0^\infty f_2(\nu)e^{-\nu}d\nu \quad (32)$$

with $f_j(\nu)$ given in (33). The integral (32) can be computed by Gauss-Laguerre integration and yields [29]

$$\Phi_{I_{s_k}|\underline{\boldsymbol{\alpha}}^{(1)},d_s}(w) = \beta\sum_{i=1}^{N_p} w_i f_1(z_i) + (1-\beta)\sum_{i=1}^{N_p} w_i f_2(z_i) \quad (34)$$

Here z_i is the abscissas of the N_pth order Laguerre polynomial $L_{N_p}(z)$ with corresponding weight

$$w_i = \frac{z_i}{(N_p+1)^2 L_{N_p+1}^2(z_i)}. \quad (35)$$

The abscissas and weights of the Laguerre-Gauss quadrature and Legendre-Gauss quadrature can be computed analytically for small value of N_p. [29] gives a table of abscissas and weights for larger value of N_p. In Fig. 1, the exact characteristic function of self interference along with its approximations by Laguerre-Gauss quadrature and Legendre-Gauss quadrature in three environments based on IEEE 802.15.4a model have been presented. As previously stated, in CM2 (and CM1) channel, Laguerre-Gauss quadrature rule approximates the characteristic function quite well; while in the CM5 (and also CM3, CM4 and CM6), Legendre-Gauss quadrature method works well (note that even though at very low frequency range Laguerre curves are closer to exact characteristic function, but totally Legendre-Gauss quadrature method approximate the characteristic function of these channels much better). The plots of CM1, CM4, and CM6 are not included here due to the space limitations.

2) CF of AWGN (η): The noise term η, the real part of $\hat{\eta}$ in (19), follows a Gaussian distribution with zero mean and variance given in (20). So its characteristic function is given by

$$\Phi_\eta(w) = \exp\left(-\frac{w^2 N_f R(0) N_0 \sum_{k=0}^{K'-1}\left|\alpha_{k,0}^{(1)}\right|^2}{2}\right) \quad (36)$$

3) CF of Total Noise: Using the independence of the SI and the noise, we have

$$\Phi_{I_s+\eta}(w) = \Phi_{I_s}(w)\Phi_\eta(w) \quad (37)$$

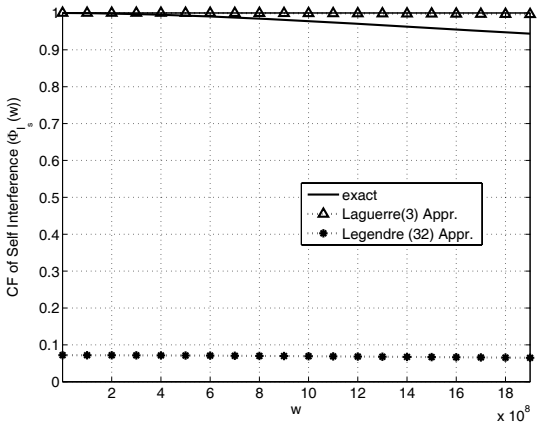

(a)

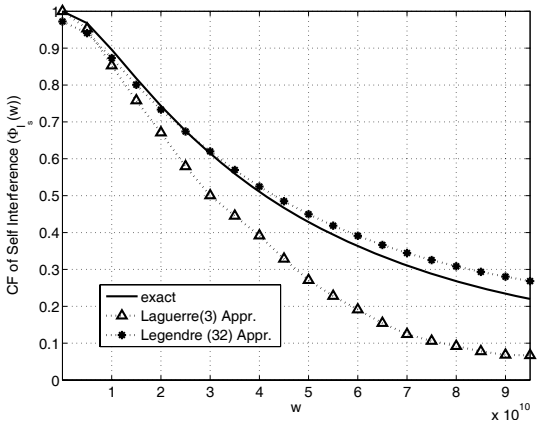

(b)

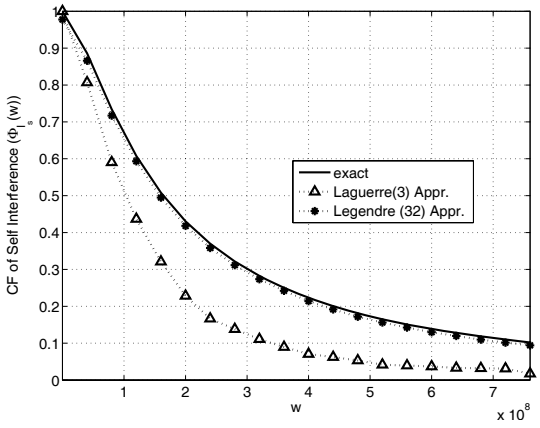

(c)

Fig. 1. The characteristic functions of Self Interference (I_s) in different IEEE 802.15.4a UWB channel. a) CM2- Residential NLOS b) CM4- Office NLOS c) CM5- Outdoor LOS

C. Bit Error Probability (BEP)

In this section, we derive an expression for the BEP of the TH-PPM UWB communication with a relay node. From (12) and (13), the decision variable Z is given by

$$Z = D^{(sd)} + I_s^{(sd)} + \eta^{(sd)} + \lambda\left(D^{(rd)} + I_s^{(rd)} + \eta^{(rd)}\right) \quad (38)$$

where the statics of $D^{(sd)}$, $I_s^{(sd)}$ and $\eta^{(sd)}$ have been obtained in (15), (17), and (20), respectively. Also, the CFs of $I_s^{(sd)}$ and $\eta^{(sd)}$ have been derived in (26) and (36), respectively. The statics and CFs of $D^{(rd)}$, $I_s^{(rd)}$ and $\eta^{(rd)}$ can be computed similarly as

$$D^{(rd)} = N_f\sqrt{E_r}\sum_{k=0}^{K'-1}\left|\alpha_{k,0}^{(3)}\right|^2 R(\delta d^r), \quad (39)$$

$$\Phi_{I_s^{(rd)}|\underline{\boldsymbol{\alpha}}^{(3)},d_r}(w) = \tilde{U}\left(N_f\sqrt{E_r}\Re\{\alpha_{K',0}^{(3)}\alpha_{K'-1,0}^{(3)\,*}\},0,\delta d_r,0\right) \cdot\prod_{k=0}^{K'-2}\tilde{U}\Big(N_f\sqrt{E_r}\Re\{\alpha_{k+1,0}^{(3)}\alpha_{k,0}^{(3)*}\},N_f\sqrt{E_r}\Re\{\alpha_{k,0}^{(3)}\alpha_{k+1,0}^{(3)\,*}\},\delta d_r,\delta d_r\Big), \quad (40)$$

and

$$\Phi_{\eta^{(rd)}}(w) = \exp\left(-\frac{w^2N_fR(0)N_0\sum_{k=0}^{K'-1}\left|\alpha_{k,0}^{(3)}\right|^2}{2}\right). \quad (41)$$

Taking into account the symmetrical property, the average probability of error for TH-PPM-UWB communication with a relay node conditioned on the channel gains $\underline{\boldsymbol{\alpha}} = \left(\underline{\boldsymbol{\alpha}}^{(1)},\underline{\boldsymbol{\alpha}}^{(2)},\underline{\boldsymbol{\alpha}}^{(3)}\right)$ is equal to the probability of error conditioned on bit "0" being sent and is given by (42), shown at the bottom of the page.

where $\Xi^{(1)} \triangleq \sum_{k=0}^{K'-1}\left|\alpha_{k,0}^{(1)}\right|^2$, $\Xi^{(3)} \triangleq \sum_{k=0}^{K'-1}\left|\alpha_{k,0}^{(3)}\right|^2$ and ϵ is the probability of incorrect decoding at the relay which is given by

$$\epsilon = \mathbb{P}\left(I_s^{(sr)} + \eta^{(sr)} \le -N_f\sqrt{E_s}R(0)\Xi^{(2)}\middle| d_s = 0,\underline{\boldsymbol{\alpha}}^{(2)}\right) \quad (43)$$

with $\Xi^{(2)} \triangleq \sum_{k=0}^{K'-1}\left|\alpha_{k,0}^{(2)}\right|^2$. The characteristic functions $\Phi_{I_s^{(sr)}|\underline{\boldsymbol{\alpha}}^{(2)},d_s}$ and $\Phi_{\eta^{(sr)}}$ are obtained similar to (40) and (41), respectively. Define $\Upsilon_{i,j} = I_s^{(sd)} + \eta^{(sd)} + \lambda I_s^{(rd)} + \lambda\eta^{(rd)}$ conditioned on $d_s = i$ and $d_r = j$; then the CF of $\Upsilon_{i,j}$ can be expressed as

$$\Phi_{\Upsilon_{i,j}|\underline{\boldsymbol{\alpha}}}(w) = \Phi_{I_s^{(sd)}|\underline{\boldsymbol{\alpha}}^{(1)},i}(w)\Phi_{\eta^{(sd)}}(w)\Phi_{I_s^{(rd)}|\underline{\boldsymbol{\alpha}}^{(3)},j}(\lambda w)\Phi_{\eta^{(rd)}}(\lambda w) \quad (44)$$

Now, we can rewrite (42) as

$$\begin{aligned}P_e &= (1-\epsilon)\mathbb{P}\left(\Upsilon_{0,0} \le -N_f\sqrt{E_s}R(0)\left(\Xi^{(1)} + \lambda\sqrt{\frac{E_r}{E_s}}\Xi^{(3)}\right)\right)\\ &\quad + \epsilon\,\mathbb{P}\left(\Upsilon_{0,1} \le -N_f\sqrt{E_s}R(0)\left(\Xi^{(1)} - \lambda\sqrt{\frac{E_r}{E_s}}\Xi^{(3)}\right)\right)\\ &= (1-\epsilon)F_{\Upsilon_{0,0}}\left(-N_f\sqrt{E_s}R(0)\left(\Xi^{(1)} + \lambda\sqrt{\frac{E_r}{E_s}}\Xi^{(3)}\right)\right)\\ &\quad + \epsilon\,F_{\Upsilon_{0,1}}\left(-N_f\sqrt{E_s}R(0)\left(\Xi^{(1)} - \lambda\sqrt{\frac{E_r}{E_s}}\Xi^{(3)}\right)\right) \quad (45)\end{aligned}$$

where $F_{\Upsilon_{i,j}}$ denotes the cumulative density function (cdf) of $\Upsilon_{i,j}$. Finally, using the Gil-Pelaez theorem [30], which relates the cdf of a random variable with its CF, P_e can be expressed as

$$\begin{aligned}P_e|\underline{\boldsymbol{\alpha}} &= 1 - \frac{(1-\epsilon)}{\pi}\int_0^\infty \frac{\Im\left\{e^{jwu_0}\Phi_{\Upsilon_{0,0}|\underline{\boldsymbol{\alpha}}}(w)\right\}}{w}dw\\ &\quad - \frac{\epsilon}{\pi}\int_0^\infty \frac{\Im\left\{e^{jwu_1}\Phi_{\Upsilon_{0,1}|\underline{\boldsymbol{\alpha}}}(w)\right\}}{w}dw \quad (46)\end{aligned}$$

where $\Im\{\cdot\}$ denotes the imaginary part and

$$u_0 = N_f\sqrt{E_s}R(0)\left(\Xi^{(1)} + \lambda\sqrt{\frac{E_r}{E_s}}\Xi^{(3)}\right), \quad (47)$$

$$u_1 = N_f\sqrt{E_s}R(0)\left(\Xi^{(1)} - \lambda\sqrt{\frac{E_r}{E_s}}\Xi^{(3)}\right), \quad (48)$$

and

$$\epsilon = \frac{1}{2} - \frac{1}{\pi}\int_0^\infty \frac{\Im\left\{e^{jwu_\epsilon}\Phi_{I_s^{(sr)}|\underline{\boldsymbol{\alpha}}^{(2)},0}(w)\Phi_{\eta^{(sr)}}(w)\right\}}{w}dw \quad (49)$$

with

$$u_\epsilon = N_f\sqrt{E_s}R(0)\Xi^{(2)}. \quad (50)$$

$$f_j(\nu) = e^{jwN_f\sqrt{E_s}\left(\Re\{\alpha_{k+1,0}^{(1)}\alpha_{k,0}^{(1)\,*}\}R(\frac{\nu}{\lambda_j}+\delta d^s)+\Re\{\alpha_{k,0}^{(1)}\alpha_{k+1,0}^{(1)\,*}\}R(-\frac{\nu}{\lambda_j}+\delta d^s)\right)} \quad j = 1,2 \quad (33)$$

$$\begin{aligned}P_e|\underline{\boldsymbol{\alpha}} &= \mathbb{P}\left(Z \le 0|d_s = 0,\underline{\boldsymbol{\alpha}}\right) = \mathbb{P}\left(I_s^{(sd)} + \eta^{(sd)} + \lambda I_s^{(rd)} + \lambda\eta^{(rd)} \le -D^{(sd)} - \lambda D^{(rd)}\middle| d_s = 0,\underline{\boldsymbol{\alpha}}\right)\\ &= (1-\epsilon)\mathbb{P}\left(I_s^{(sd)} + \eta^{(sd)} + \lambda I_s^{(rd)} + \lambda\eta^{(rd)} \le -N_f\sqrt{E_s}R(0)\left(\Xi^{(1)} + \lambda\sqrt{\frac{E_r}{E_s}}\Xi^{(3)}\right)\middle| d_s = 0,\underline{\boldsymbol{\alpha}}\right)\\ &\quad + \epsilon\,\mathbb{P}\left(I_s^{(sd)} + \eta^{(sd)} + \lambda I_s^{(rd)} + \lambda\eta^{(rd)} \le -N_f\sqrt{E_s}R(0)\left(\Xi^{(1)} - \lambda\sqrt{\frac{E_r}{E_s}}\Xi^{(3)}\right)\middle| d_s = 0,\underline{\boldsymbol{\alpha}}\right) \quad (42)\end{aligned}$$

To obtain the unconditional BEP, we should take the expected value of (46), respect to $\alpha_{0,0}^{(j)},\ldots,\alpha_{K',0}^{(j)}$, for $j=1,2,3$. To compute this multi-dimensional integration, one approach is to phrase the multiple integral as repeated one-dimensional integrals by appealing to Fubini's theorem [29] and then compute each integral using the Gaussian quadrature rule described in the previous subsection. However, this approach makes the function evaluations grow exponentially as the number of dimensions increases. Monte Carlo (quasi-Monte Carlo) method and Sparse grids method are known to overcome this so-called curse of dimensionality. Monte Carlo method is easy to apply to multi-dimensional integrals, and may yield greater accuracy for the same number of function evaluations than repeated integrations using one-dimensional methods. Sparse grids, developed for the quadrature of high dimensional functions, is based on a one dimensional quadrature rule, but performs a more sophisticated combination of univariate results. For numerical evaluations, we have used Monte Carlo method to compute this multi-dimensional integration.

D. Approximation for the BEP of UWB Channel with a Relay Node

In some scenarios with a good assumption it can be assumed that we deal with a completely resolvable paths, namely $|\tau_{k,\ell}^{(j)}-\tau_{k',\ell'}^{(j)}|\geq T_c, \forall(k,\ell)\neq(k',\ell')$ [14]. UWB systems with a very large bandwidth (very small T_p) and some defined channels in IEEE 802.15.4a standard such as residential environments can satisfy this situation. In this case, the self interference term (I_s) in the decision variable is fully omitted and the decision variable Z in (38) is reduced to

$$Z=N_f\sqrt{E_s}\Xi^{(1)}R(\delta d^s)+\lambda N_f\sqrt{E_r}\Xi^{(3)}R(\delta d^r)+\eta^{(sd)}+\lambda\eta^{(rd)} \quad (51)$$

where $\Xi^{(1)}$ and $\Xi^{(1)}$ have been defined in (43). Conditioning upon $\underline{\boldsymbol{\alpha}}$, the decision statics Z is Gaussian random variable and the conditional probability of error is simply obtained as

$$\begin{aligned} P_e|\underline{\boldsymbol{\alpha}} &= (1-\epsilon)Q\left(\sqrt{\frac{N_fR(0)}{N_0}\frac{\left(\sqrt{E_s}\Xi^{(1)}+\lambda\sqrt{E_r}\Xi^{(3)}\right)^2}{\Xi^{(1)}+\lambda^2\Xi^{(3)}}}\right) \\ &\quad + \epsilon\ Q\left(\sqrt{\frac{N_fR(0)}{N_0}\frac{\left(\sqrt{E_s}\Xi^{(1)}-\lambda\sqrt{E_r}\Xi^{(3)}\right)^2}{\Xi^{(1)}+\lambda^2\Xi^{(3)}}}\right) \quad (52)\end{aligned}$$

where $Q(x)=1/\sqrt{2\pi}\int_x^\infty e^{-t^2/2}\ dt$. In the case of equal transmit powers of the source and relay nodes, *i.e.,*$E_s=E_r$, we have

$$\begin{aligned} P_e|\underline{\boldsymbol{\alpha}} &= (1-\epsilon)Q\left(\sqrt{\frac{E_sN_fR(0)}{N_0}\frac{\left(\Xi^{(1)}+\lambda\Xi^{(3)}\right)^2}{\Xi^{(1)}+\lambda^2\Xi^{(3)}}}\right) \\ &\quad + \epsilon\ Q\left(\sqrt{\frac{E_sN_fR(0)}{N_0}\frac{\left(\Xi^{(1)}-\lambda\Xi^{(3)}\right)^2}{\Xi^{(1)}+\lambda^2\Xi^{(3)}}}\right) \quad (53)\end{aligned}$$

In the above equations, ϵ is given by

$$\begin{aligned} \epsilon &= \mathop{\mathbb{E}}_{\underline{\boldsymbol{\alpha}}^{(2)}}\left\{Q\left(\sqrt{\frac{E_sN_fR(0)\Xi^{(2)}}{N_0}}\right)\right\} \\ &= \mathop{\mathbb{E}}_{c,m_t}\left\{\frac{1}{2\sqrt{\pi}}\frac{\sqrt{c}}{(1+c)^{m_t+\frac{1}{2}}}\frac{\Gamma(m_t+\frac{1}{2})}{\Gamma(m_t+1)}\right. \\ &\quad \left.\cdot\ {}_2F_1\left(1,m_t+\frac{1}{2};m_t+1;\frac{1}{1+c}\right)\right\} \quad (54)\end{aligned}$$

In obtaining the second equality of (54), we have used the fact that the sum of independent Nakagami coefficients in power terms, namely $\Xi^{(2)}=\sum_{k=0}^{K'-1}\left|\alpha_{k,0}^{(2)}\right|^2$, can be approximated by an equivalent gamma distribution with the following parameters [31], [32]

$$\Omega_t\simeq\sum_{k=0}^{K'-1}\Omega_{k,0}^{(2)},\qquad m_t\simeq\frac{\left(\sum_{k=0}^{K'-1}\Omega_{k,0}^{(2)}\right)^2}{\sum_{k=0}^{K'-1}\frac{\Omega_{k,0}^{(2)\,2}}{m_{k,0}^{(2)}}} \quad (55)$$

In (54), c is defined as $c\triangleq\frac{E_sN_fR(0)}{2N_0}\frac{\Omega_t}{m_t}$ and $\Gamma(\cdot)$ and ${}_2F_1(\cdot,\cdot;\cdot;\cdot)$ are the Gamma and Gauss hypergeometric functions, respectively [29].

IV. Numerical Results and Discussion

In this section we present some numerical examples, aiming to investigate the theoretical BEP formulas derived. Monte-Carlo computer simulations are carried out to validate our analytical derivations and illustrate the accuracy of the approximation used in the previous sections. For numerical evaluations and simulation purposes, in all the ensuing plots, the second derivative of a Gaussian pulse with an approximated duration of .7 ns is employed and δ is set to .15 ns.

The channels between the nodes adopt the UWB multipath model by IEEE 802.15.4a Task Group. The simulations are carried out mainly in CM2 which corresponds to the residential NLOS environment. The channel bandwidth is set to be 3 GHz. The values of the channel parameters have been taken from [12]. In our plots, we have considered the pathloss as a function of distance and ignored its frequency dependency. We have assumed that the transmitter power decays according to the "power law" which is described in dB by

$$\mathrm{PL}(d)=\mathrm{PL}_0+10\mathrm{n}\log(\frac{d}{d_0}), \quad (56)$$

where the reference distance d_0 is set to 1 m, PL_0 is the path-loss at the reference distance and n is the path-loss exponent, which also depends on the environment and whether or not LOS exists. The distance d_1 between the source and the destination has been set to 3 m, and we assume that the relay node is exactly in the middle between them. Furthermore, it is assumed that the transmitted powers by the source and the relay node are the same and at most equal to the maximum allowed power for the UWB systems which is stipulated by FCC ($-41.3\,\mathrm{dBm/MHz}$). Considering (56), the maximum allowed transmitted power, and assuming the noise power spectral density of $-114\,\mathrm{dBm/MHz}$, the maximum received SNRs at distance 3 m for CM1–CM6 become 20.3 dB, 2.1 dB, 29.5 dB, 0.1523 dB, 18.7 dB and -12.23 dB, respectively. In all the ensuing plots, we have assumed equal average fading power of 1 for all S-R, S-D and R-D links (averaged over all the different random processes) and finally a rake receiver with 5 fingers ($K'=5$) and a combination factor of $\lambda=\frac{\mathrm{PL}_3}{\mathrm{PL}_1}$ are assumed in our evaluation.

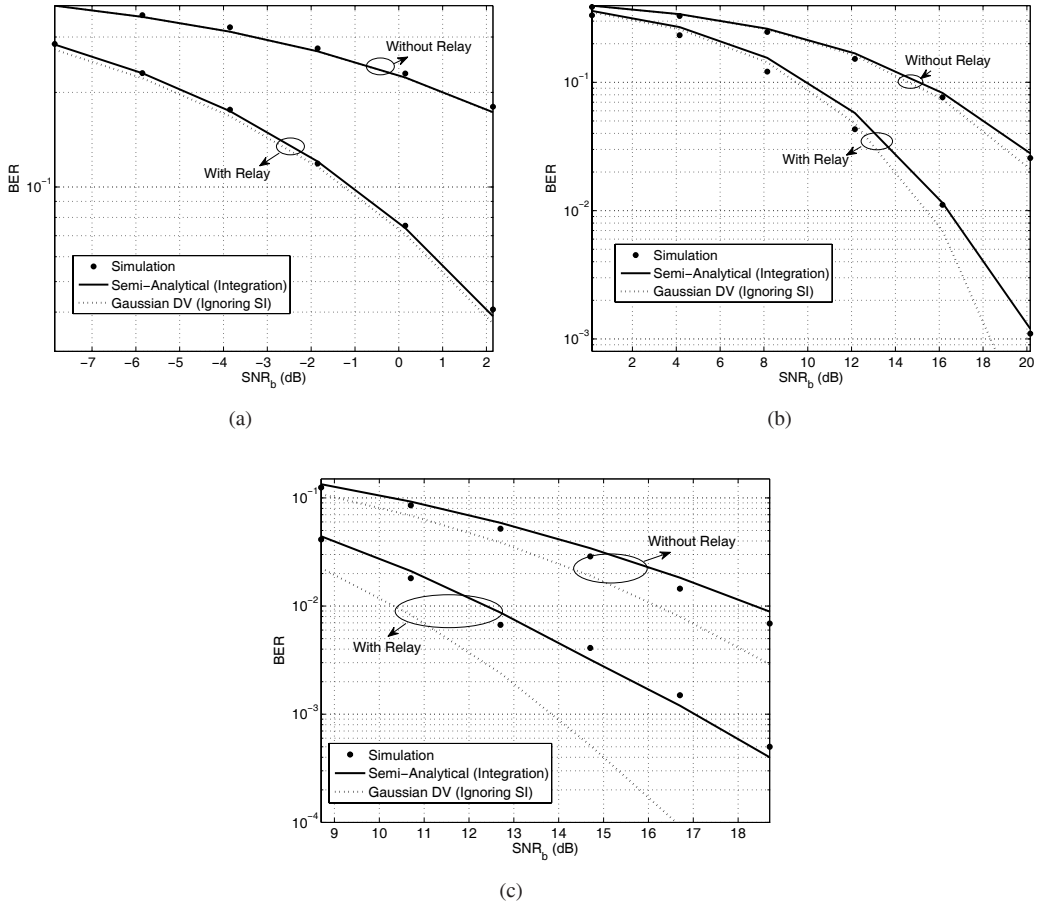

Fig. 2. Average BEP of UWB-linked relay network vs. bit SNR. a)under CM2 b)under CM4 c)under CM5

Fig. 2(a) shows the BEP of the UWB communication with a relay node computed using the CF method (46)(dash line) as well as the BEPs obtained by ignoring self interference (Gaussian decision variable)(dot line) and simulation (stars) in residential NLOS scenario(CM2). This figure also contains similar plots for the BEPs of the conventional UWB transmission (without a relay node). As can be realized, the BEP performance improves significantly using a relay node and this superiority increases with the SNR. In this plot SNR means the power spectral density ratio between the received signal and noise of direct path between source and destination nodes. Also, as the figure shows, simulation results are close to the derived analytic BEP values, with minor deviations due to the approximations involved in describing the self interference term (17). This agreement exists in all range of the considered SNR which validates our theoretical analysis. Gaussian approximation (53) is in good agreement with the exact analysis in this environment too (Fig. 2(a)). Fig. 2(b) and 2(c) contain similar curves for office NLOS and outdoor LOS scenarios (CM4 and CM5). Note that Gaussian assumption will not work well for all 8 kinds of IEEE 802.15.4a environments. In fact two factors determine the accuracy of Gaussian assumption obtained from the ignoring of the self interference. First one is the number of interfered pulses and the second one is the power of each path. In the NLOS scenarios (CM2, CM4, and CM6) as the power of the received paths are usually weak, we expect that we can use this approximation with a good precision and Fig. 2(a) and Fig. 2(b) confirm this expectation for CM2 and CM4, respectively. We also simulated for CM6 channel and it exhibited similar behavior. Note that as the the numbers of interfered pulses in CM4 and CM6 are significant compared to CM2, the Gaussian assumption in these channels is not as good as in CM2 when the transmitted signal power approaches to its maximum allowed value specified by FCC. However, the gap is not high and in the allowed transmitted power range the Gaussian assumption can be still used confidently for CM4 and CM6, too. We should point out that the last point in Fig. 2(b) is for the case of the power 20 dB above the maximum allowed power by FCC. But in the LOS scenario we deal with stronger paths. Therefore in these cases SI can be ignored in the decision statics only if the number of interfering pulses is small. We examined and observed that this approximation works well only for CM1. So as Fig. 2(c) shows, Gaussian assumption underestimates the BEP for the left two environments, namely office LOS (CM3) and outdoor LOS (CM5), in which more SI is introduced. This phenomenon is demonstrated more clearly in Fig. 3, where the characteristic functions of SI, AWGN, and total

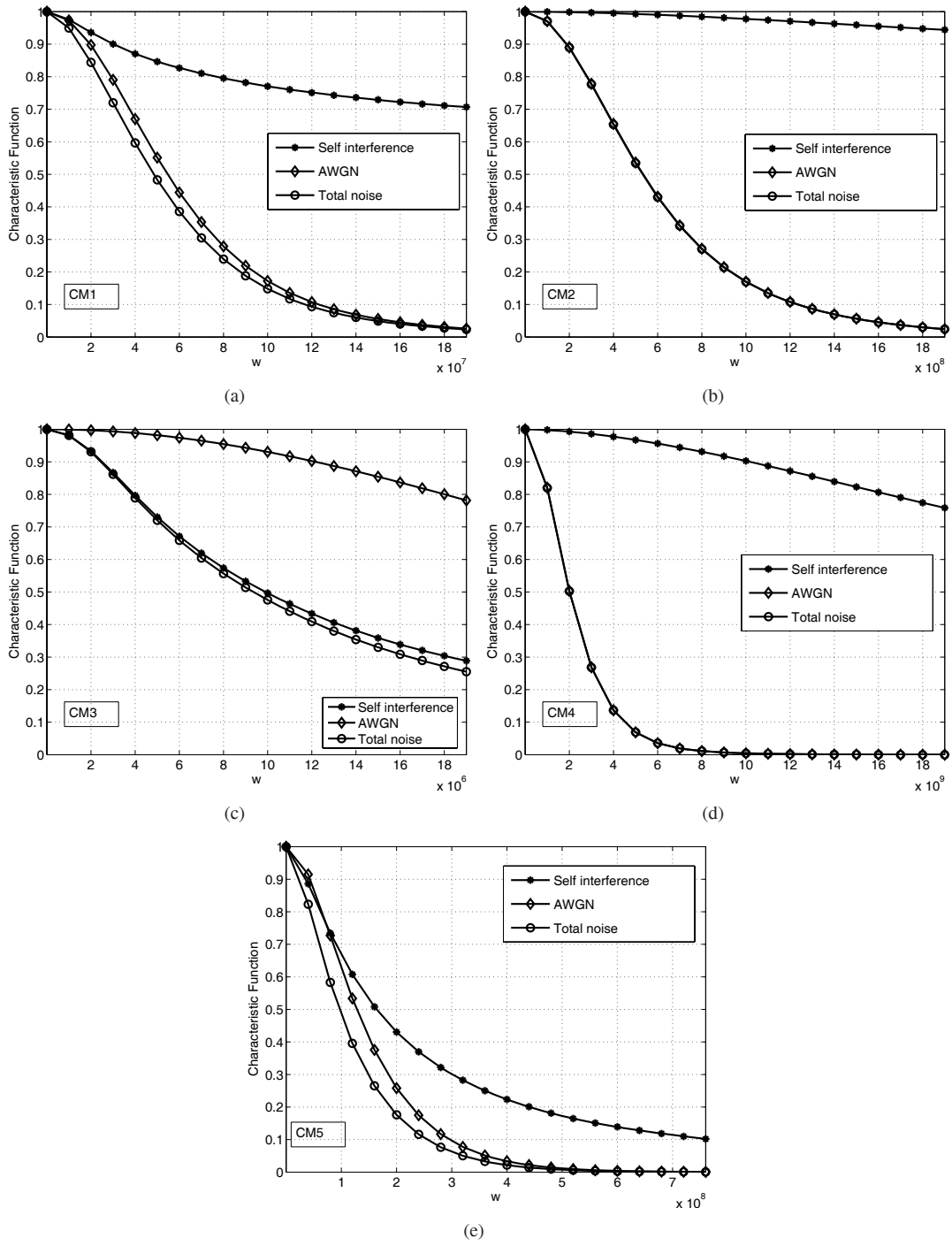

Fig. 3. The characteristic functions of AWGN (η), self interference (I_s), and total noise $(I_s + \eta)$ in different IEEE 802.15.4a UWB channel. a) CM1- Residential LOS b) CM2- Residential c) CM3- Office LOS d) CM4- Office NLOS e) CM5- Outdoor LOS

noise have been presented to help interpreting this results. From Fig. 3, in CM1 and CM2 scenarios the characteristic function of the AWGN is the nearest curve to the characteristic function of the total noise. In other words, the total noise is dominated by AWGN in these environments and therefore self interference term can be ignored safely. Similar confirmation holds for CM4 and CM6 channels. The plots of CM6 are not included here due to the space limitation. But in the other environments (CM3 and CM5) Φ_{total} is apparently different from Φ_η and it almost overlaps with the characteristic function of self interference, since SI becomes dominant. Accordingly, the Gaussian approximation method does not work well in these scenarios.

In Fig. 2, the BEP curves are versus the SNR per bit. In the other words, the total energy of bit has been splitted equally among pulses transmitted in N_f frames and as there does not exist any multiple access interference the performance does not change by N_f. Now, we relax the restriction on the total

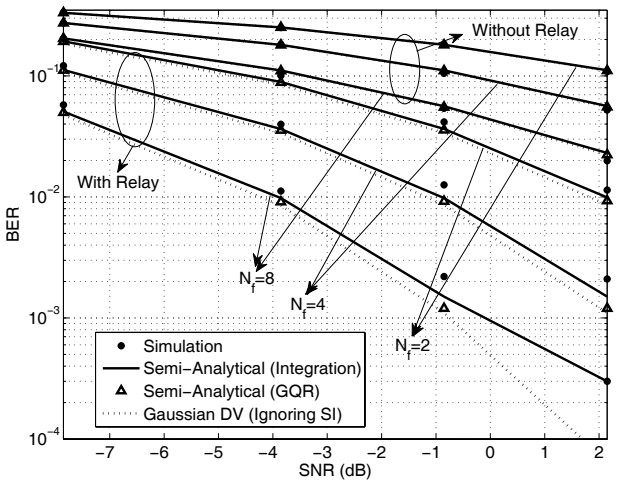

Fig. 4. Average BEP of UWB-linked relay network vs. pulse SNR for $N_f = 2, 4, 8$.

power of the symbol and constrain this restriction on each transmitted pulse and let the power of each transmitted pulse to be at most equal to the maximum allowed power determined by FCC. In this case we reach to the better performance by increase of N_f while the FCC regulation is still met. In Fig. 4 we have considered this restriction, where for different value of N_f the BEP performance of the system in CM2 channel versus direct line transmitted pulse signal to noise ratio has been shown. As we expect, due to the energy per symbol increment, the BEP decreases by N_f and again we have a significant improvement in the system performance using a relay node and this improvement is more impressive at larger value of N_f and SNR. In this figure, the BEP results have been also compared with those employing Gaussian quadrature rule, i.e., (27). For the analyzed configurations, GQR shows an almost perfect agreement with simulated curves. The number of points for the Laguerre Gaussian rule is 3. The choice of the number of points in the GQR is a crucial aspect in order to obtain reliable results. In principle, the truncation error can be made as small as desired, by increasing the number of abscissae and weights of the quadrature rule. However, this is not sufficient in practice, since these abscissae and weights are not known with infinite accuracy. This can make some gaps between the exact value and approximated ones. We can observe this phenomena on the curves related to $N_f = 8$. In Fig. 4 the curves based on the Gaussian approximation are also provided. As it is obvious the GA fails to predict the error-rate floor of the system (caused by the interference) on CM2 links as N_f increases. Our investigation reveals that in the case of constraint on each transmitted pulse, GA is not reliable when N_f or SNR increases.

V. Conclusion

We derived the BEP of a DF relay network employing UWB links developed by IEEE 802.15.4a standards between its three nodes. To this end, we have used Gaussian quadrature numerical method to approximate the CF of self interference appeared in decision variable statics. Numerical results have shown that significant improvement in the BEP of impulse radio UWB system is obtained by adding a relay node. Our further investigations have indicated that there is an optimum position for the relay node between the source and the destination, in which the BEP is minimized. The analytical expressions were also validated by computer simulations. This confirmed the accuracy of the approximations used in obtaining the BEP.

References

[1] M. Win and R. Scholz, "Ultra-wide bandwidth time-hopping spread-spectrum impulse radio for wireless multiple-access communications," *IEEE Trans. Commun.*, vol. 48, pp. 679-691, Apr. 2000.

[2] W. P. Siriwongpairat, W. Su, Z. Han, and K. J. R. Liu, "Employing cooperative diversity for performance enhancement in UWB communication systems," in *Proc. IEEE Wireless Commun. Netw. Conf. (WCNC)*, vol. 4, 2006, pp. 1854-1859.

[3] A. Jamshidi and M. Nasiri-Kenari, "Performance analysis of transmitter-side cooperationŰreceiver-side-relaying schemes for heterogeneous sensor networks," *IEEE Trans. Veh. Technol.*, vol. 57, no. 3, pp. 1548-1563, May 2008.

[4] C. Li, G. Yue, M. A. Khojastepour, X. Wang, and M. Madihian, "LDPC-coded cooperative relay systems: performance analysis and code design," *IEEE Trans. Commun.*, vol. 56, no. 3, pp. 485-496, Mar. 2008.

[5] E. van-der Meulen, "Three-terminal communication channels," *Adv. Appl. Prob.*, vol. 3, pp. 120-154, 1971.

[6] D. Chen and J. N. Laneman, "Modulation and demodulation for cooperative diversity in wireless systems," *IEEE Trans. Wireless Commun.*, vol. 5, no. 7, pp. 1785-1794, July 2006.

[7] I.-H. Lee and D. Kim, "BER analysis for decode-and-forward relaying in dissimilar Rayleigh fading channels," *IEEE Commun. Lett.*, vol. 11, no. 1, pp. 52-54, Jan. 2007.

[8] A. Sendonaris, E. Erkip, and B. Aazhang, "User cooperation diversity—part I: system description," *IEEE Trans. Commun.*, vol. 51, no. 11, pp. 1927-1938, Nov. 2003.

[9] G. Kramer, M. Gastpar, and P. Gupta, "Cooperative strategies and capacity theorems for relay networks," *IEEE Trans. Inf. Theory*, vol. 51, no. 9, pp. 3037-3063, Sept. 2005.

[10] J. N. Laneman, D. N. C. Tse, and G. W. Wornell, "Cooperative diversity in wireless networks: efficient protocols and outage behavior," *IEEE Trans. Inf. Theory*, vol. 50, no. 12, pp. 3062-3080, Dec. 2004.

[11] J. N. Laneman and G. W. Wornell, "Distributed space-time-coded protocols for exploiting cooperative diversity in wireless networks," *IEEE Trans. Inf. Theory*, vol. 49, no. 10, pp. 2415-2425, Oct. 2003.

[12] A. F. Molisch, C. C. Chong, B. Kannan, S. Emami, A. Fort, J. Karedal, and U. G. Schuster, "802.15.4a channel model subgroup final report, IEEE 802.15-04-0535-00-004a," Berlin, Germany, Sept. 2004.

[13] B. Hu and N. C. Beaulieu, "Accurate evaluation of multiple-access performance in TH-PPM and TH-BPSK UWB systems," *IEEE Trans. Commun.*, vol. 52, no. 10, pp. 1758-1766, Oct. 2004.

[14] J. Choi and W. Stark, "Performance of ultra-wideband communications with suboptimal receivers in multipath channels," *IEEE J. Sel. Areas Commun.*, vol. 20, no. 9, pp. 1754-1766, Dec. 2002.

[15] S. Niranjayan, A. Nallanathan, and B. Kannan, "Modeling of multiple access interference and BER derivation for TH and DS UWB multiple access systems," *IEEE Trans. Wireless Commun.*, vol. 5, no. 10, pp. 2794-2804, Oct. 2006.

[16] W. Cao, A. Nallanathan, and C. C. Chai, "Exact BER analysis of DS PPM UWB multiple access system in lognormal multipath fading channels," in *Proc. IEEE Globecom Conf.*, Nov. 2006, pp. 1-5.

[17] L. A. Gubner and K. Hao, "A computable formula for the average bit error probability as a function of window size for the IEEE 802.15.3a UWB channel model," *IEEE Trans. Microw. Theory Technol.*, vol. 54, no. 4, pp. 1762-1768, Apr. 2006.

[18] W.-C. Liu and L.-C. Wang, "BER analysis in a generalized UWB frequency selective fading channel with randomly arriving clusters and rays," in *Proc. IEEE Int. Conf. Commun.*, June 2007.

[19] Z. Ahmadian and L. Lampe, "Performance analysis of the IEEE 802.15.4a UWB system," *IEEE Trans. Commun.*, vol. 57, no. 5, pp. 1474-1485, May 2009.

[20] C. Abou-Rjeily, N. Daniele, and J.-C. Belfiore, "On the decode-and-forward cooperative diversity with coherent and non-coherent UWB systems," in *Proc. IEEE Int. Conf. Ultra-Wideband*, Sept. 2006, pp. 435-440.

[21] ——, "On the amplify-and-forward cooperative diversity with time-hopping ultra-wideband communications," *IEEE Trans. Commun.*, vol. 56, no. 4, pp. 630-641, Apr. 2008.
[22] Z. Zeinalpour-Yazdi, M. Nasiri-Kenari, B. Aazhang, J. Wehinger, and C. F. Mecklenbräuker, "Bounds on the delay-constrained capacity of UWB communication with a relay node," *IEEE Trans. Wireless Commun.*, vol. 8, no. 5, pp. 2265-2273, May 2009.
[23] A. Saleh and R. Valenzuela, "A statistical model for indoor multipath propagation," *IEEE J. Sel. Areas Commun.*, vol. 5, no. 2, pp. 128-137, Feb. 1987.
[24] M. Z. Win, "Spectral density of random time-hopping spread spectrum UWB signals with uniform timing jitter," *IEEE Commun. Lett.*, vol. 2, pp. 36-38, Feb. 1998.
[25] W. P. Siriwongpairat, M. Olfat, and K. J. R. Liu, "Performance analysis of time hopping and direct sequence UWB space-time systems," in *Proc. IEEE Globecom Conf.*, Nov. 2004.
[26] H. Chen, M. Guizani, C. Tsai, Y. Xiao, R. Fantacci, and H. Sharif, "Pulse waveform dependent BER analysis of a DS-CDMA UWB radio under multiple access and multipath interferences," *IEEE Trans. Wireless Commun.*, vol. 6, no. 6, pp. 2338-2347, June 2007.
[27] A. Sendonaris, E. Erkip, and B. Aazhang, "User cooperation diversity—part II: implementation aspects and performance analysis," *IEEE Trans. Commun.*, vol. 51, no. 11, pp. 1939-1948, Nov. 2003.
[28] W. P. Siriwongpairat, W. Su, M. Olfat, and K. J. R. Liu, "Multiband-OFDM MIMO coding framework for UWB communication systems," *IEEE Trans. Signal Process.*, vol. 54, no. 1, pp. 214-224, Jan. 2006.
[29] M. Abramowitz and I. A. Stegun, *Handbook of Mathematical Functions with Formulas, Graphs, and Mathematical Tables*. New York: Dover, 1965.
[30] J. Gil-Pelaez, "Note on the inversion theorem," *Biometrika*, vol. 38, pp. 481-482, Dec. 1951.
[31] J. Reig and N. Cardona, "Approximation of outage probability on Nakagami fading channels with multiple interference," *Electron. Lett.*, vol. 36, no. 19, pp. 1649-1650, Sept. 2000.
[32] M. Nakagami, "The m-distribution—a general formula of intensity distribution of rapid fading," *Statistical Methods in Radio Wave Propagation: Proceedings of a Symposium held at the University of California*, W. G. Hoffman, editor, pp. 3-36, Pergamon Press, 1960.

Zolfa Zeinalpour-Yazdi (S'09) received her B.Sc. and M.Sc. both in Electrical Engineering from Sharif University of Technology, Tehran, Iran, in 2002 and 2004, respectively. She is currently a Ph.D. student in the wireless research group at Sharif University of Technology. She has held visiting research at ftw. Telecommunication Research Center, Vienna, Austria in 2006. Her research interests are in wireless communications and networking with special emphasis on ultra-wideband systems and cooperative communications.

Masoumeh Nasiri-Kenari (S'90-M'94) received the B.S and M.S. degrees in electrical engineering from Isfahan University of Technology, Isfahan, Iran, in 1986 and 1987, respectively, and the Ph.D. degree in electrical engineering from the University of Utah, Salt Lake City, in 1993.

From 1987 to 1988, she was a Technical Instructor and Research Assistant at Isfahan University of Technology. Since 1994, she has been with the Department of Electrical Engineering, Sharif University of Technology, Tehran, Iran, where she is now a Professor.

Dr. Nasiri-Kenari also serves as the head of Wireless Lab. of Advanced Communications Research Institute, Sharif University of Technology. From 1999-2001, She was a Co-Director of the Advanced Communication Science Research Laboratory, Iran Telecommunication Research Center, Tehran, Iran. Her current research interests are in wireless communication systems, error correcting codes, and optical communication systems.

Behnaam Aazhang (S'82-M'82-SM'91-F'99) received his B.S. (with highest honors), M.S., and Ph.D. degrees in Electrical and Computer Engineering from University of Illinois at Urbana-Champaign in 1981, 1983, and 1986, respectively.

From 1981 to 1985, he was a Research Assistant in the Coordinated Science Laboratory, University of Illinois. In August 1985, he joined the faculty of Rice University, Houston, Texas, where he is now the J.S. Abercrombie Professor, and Chair of the Department of Electrical and Computer Engineering. In addition, he holds an Academy of Finland Distinguished Visiting Professorship appointment (FiDiPro) at the Center for Wireless Communication (CWC) in the University of Oulu, Oulu, Finland. He has served as the founding director of Rice's Center for Multimedia Communications from 1998 till 2006. He has been a Visiting Professor at IBM Federal Systems Company, Houston, Texas, the Laboratory for Communication Technology at Swiss Federal Institute of Technology (ETH), Zurich, Switzerland, the Telecommunications Laboratory at University of Oulu, Oulu, Finland, the U.S. Air Force Phillips Laboratory, Albuquerque, New Mexico, and at Nokia Mobile Phones in Irving, Texas. His research interests are in the areas of communication theory, information theory, and their applications with emphasis on multiple access communications, cellular mobile radio communications, and wireless communication networks.

Dr. Aazhang is a Fellow of IEEE, a distinguished lecturer of IEEE Communication Society, and also a recipient of 2004 IEEE Communication Society's Stephen O. Rice best paper award for a paper with A. Sendonaris and E. Erkip. He has been listed in the Thomson-ISI Highly Cited Researchers and has been keynote and plenary speaker of several conferences. Dr. Aazhang is a recipient of the Alcoa Foundation Award 1993, the NSF Engineering Initiation Award 1987-1989, and the IBM Graduate Fellowship 1984-1985, and is a member of Tau Beta Pi and Eta Kappa Nu.

He is serving as the co-general chair of 2010 International Symposium on Information Theory (ISIT), in Austin, Texas. He has served on Houston Mayor's Commission on Cellular Towers 1998-2004, as the Editor for Spread Spectrum Networks of IEEE Transactions on Communications 1993-1998, the Treasurer of IEEE Information Theory Society 1995-1998, the Secretary of the Information Theory Society 1990-1993, the Publications Chairman of the 1993 IEEE International Symposium on Information Theory, San Antonio, Texas, the co-chair of the Technical Program Committee of 2001 Multi-Dimensional and Mobile Communication (MDMC) Conference in Pori, Finland, the chair of the Technical Program Committee for 2005 Asilomar Conference, Monterey, CA, the co-chair of the Technical Program Committee of International Workshop on Convergent Technologies (IWCT), Oulu, Finland, June 2005, guest editor for IEEE JOURNAL ON SELECTED AREAS OF COMMUNICATION special issue on relay and cooperative communication in 2006 and for KICS JOURNAL OF COMMUNICATION AND NETWORK (JCN) special issue on cooperative communication in 2007, the general chair of the 2006 Communication Theory Workshop, Dorado, Puerto Rico, and the co-technical program chair of 2008 WPMC in Lapland, Finland.